PHYSICAL REVIEW D **87,** 016006 (2013)

Walking technipions at the LHC

Junji Jia,[1,*] Shinya Matsuzaki,[2,†] and Koichi Yamawaki[1,‡]

[1]*Kobayashi-Maskawa Institute for the Origin of Particles and the Universe (KMI) Nagoya University, Nagoya 464-8602, Japan*

[2]*Maskawa Institute for Science and Culture, Kyoto Sangyo University, Motoyama, Kamigamo, Kita-Ku, Kyoto 603-8555, Japan*

(Received 3 July 2012; published 9 January 2013)

We calculate technipion masses of the walking technicolor by explicitly evaluating nontrivial contributions from various possible chiral breaking sources in a concrete walking technicolor setting of the one-family model. Our explicit computation of the mass and the coupling in this concrete model setting reveals that the technipions are on the order of several hundred GeV in the region to be discovered at the LHC.

DOI: 10.1103/PhysRevD.87.016006 PACS numbers: 12.60.Nz

I. INTRODUCTION

Technicolor (TC) [1–3] provides the dynamical origin of the electroweak (EW) symmetry breaking by triggering condensation of technifermion bilinear without the introduction of a fundamental Higgs boson as in the standard model (SM). However, the original version of TC [1], a naive scale-up version of QCD, has already been excluded due to the excessive flavor changing neutral currents (FCNC).

The solution to the FCNC problem was given by the walking TC having large anomalous dimension $\gamma_m = 1$ due to the scale-invariant (conformal) gauge dynamics with nonrunning coupling [4].[1] The coupling is actually slowly running (walking) in a nonperturbative sense *a la* Miransky [6]. (Subsequently, similar ideas were proposed without notion of the anomalous dimension and the scale invariance [7].) The mass of technifermion $m_F(= \mathcal{O}(1\ \text{TeV}))$ is generated dynamically in such a way that m_F near the critical coupling $\alpha \simeq \alpha_c$ can be exponentially smaller than the cutoff Λ [to be identified with the scale of the extended TC (ETC) [8,9] $\Lambda = \Lambda_{\text{ETC}} = \mathcal{O}(10^3\text{–}10^4\ \text{TeV})$], the so-called Miransky scaling [6], closely tied with the conformal phase transition [10]. Then the walking behavior extends in a wide region $m_F < p < \Lambda$. The chiral condensate is enhanced by the large anomalous dimension of technifermion bilinear operator $\gamma_m \simeq 1$, so that realistic masses of SM light fermions[2] can be realized without suffering from the FCNC problem.[3]

Such a scale-invariant dynamics may be realized in a model having a large number of technifermion flavors (N_{TF}), as exemplified by the large N_f QCD which has an approximate infrared fixed point (IRFP), the Caswell-Banks-Zaks IRFP [18] in the two-loop beta function [10,19,20]. Thanks to the IRFP, the two-loop coupling is almost nonrunning up to the intrinsic scale Λ_{TC}, an analogue of Λ_{QCD}, above which the coupling runs as in a usual asymptotically free gauge theory like QCD, and hence Λ_{TC} plays the role of the ultraviolet cutoff Λ where the infrared conformality relevant to the walking dynamics terminates. In the same way as the scale-invariant case, m_F can be generated much smaller than $\Lambda_{\text{TC}}(\gg m_F)$ *a la* Miransky scaling, and hence the nonperturbative walking regime of the coupling extends in a wide region of energy scale $m_F < p < \Lambda_{\text{TC}}$, in sharp contrast to the ordinary QCD where the intrinsic scale Λ_{QCD} plays a role of the infrared scale $\Lambda_{\text{QCD}} \sim m_F$ without the infrared conformality region. Thus the asymptotically free region $p > \Lambda_{\text{TC}}$ will be embedded in an ETC [8], $\Lambda_{\text{TC}} \sim \Lambda \sim \Lambda_{\text{ETC}}$.

As concrete realization of the walking TC, which generally needs a large number of technifermion flavors, we may consider the Farhi-Susskind one-family model [2], which consists of one family of the technifermions (techniquarks and technileptons) having the same SM gauge charges as those of the SM fermions (ordinary quarks and leptons). The global chiral symmetry breaking then gets enhanced from the minimal structure, $SU(2)_L \times SU(2)_R \to SU(2)_V$ as in the SM, to an extended one, $SU(8)_L \times SU(8)_R \to SU(8)_V$, and hence gives rise to the associated

*junjijia@kmi.nagoya-u.ac.jp
†synya@cc.kyoto-su.ac.jp
‡yamawaki@kmi.nagoya-u.ac.jp

[1]Such a solution by the large anomalous dimension was suggested in an earlier paper [5] based on an assumption on the existence of a theory having a large anomalous dimension and ultraviolet fixed point without concrete dynamics and concrete value of the anomalous dimension.

[2]The top mass is quite hard to be reproduced by the walking TC with anomalous dimension $\gamma_m \simeq 1$. Other dynamics such as the top quark condensate [11] may be required. However, it was found [12] that if we include additional four-fermion interactions like strong ETC, the anomalous dimension becomes much larger $1 < \gamma_m < 2$, which can boost the ETC-origin mass to be arbitrarily large up to the technifermion mass scale ("strong ETC model"). (Subsequently the same effects were also noted without the concept of the anomalous dimension [13].)

[3]Another problem of the TC as a QCD scale-up is the electroweak constraints, the so-called S and T parameters. This may also be improved in the walking TC [14–16]. Even if the walking TC in isolation cannot overcome this problem, there still exists a possibility that the problem may be resolved in the combined dynamical system including the SM fermion mass generation such as ETC dynamics [8,9], in much the same way as the solution ("ideal fermion delocalization") [17] in the Higgsless models which simultaneously adjust S and T parameters by incorporating the SM fermion mass profile.

60 pseudo Nambu-Goldstone bosons ("technipions"). (Three of the total 63 are eaten by the SM weak bosons.) Probing those technipions at the collider experiments is thus necessary for discovering the walking TC.

The presence of the wide walking region implies approximate scale invariance, which is broken spontaneously by the technifermion mass generation at the same time the chiral symmetry is broken. The associated pseudo-Nambu Goldstone boson "technidilaton" [4] therefore emerges as a light composite scalar formed as a technifermion and antitechnifermion bound state. The walking low-lying spectra would thus consist of technipions and technidilaton ("walking pseudos") whose collider signatures would therefore serve as definite benchmarks toward the discovery of the walking TC.

Actually, the technidilaton signatures at the LHC have recently been discussed [21–23] in comparison with the SM Higgs. It was shown that the characteristic signatures are seen through the diphoton channel either at around 125 GeV, consistently with the currently reported diphoton excess [24], or above 600 GeV as a nonresonant excess in a higher energy region of the diphoton invariant mass distribution.

In Ref. [25], on the other hand, the current LHC limits on technipions have also been discussed focusing on isospin-color singlet technipion (denoted as P^0 in the original literature [2]) in the diphoton and tau lepton pair channels, taking the technipion mass as a free parameter. In the case of the one-family walking TC, however, the technipion masses can be pulled up to a higher scale than that expected from naive scaling of QCD [3]. Such a naively believed folklore in the technipion phenomenology should be clarified by the explicit estimate of masses and couplings of techni-pions incorporating the essential features of walking dynamics, which would also find out more relevant parameter regions to search for walking technipions at the LHC. In fact such *explicit* overall calculations of the masses and the couplings in the concrete TC model geared to the LHC phenomenology have not been done so far.[4]

[4]Actually, it was shown in the walking TC [4] that the technipion mass of ETC origin is enhanced by the anomalous dimension $\gamma_m \simeq 1$ due to the scale-invariant dynamics of the ladder Schwinger-Dyson equation. Such an enhancement by the large anomalous dimension was suggested in an earlier paper [5] without concrete dynamics and concrete value of the anomalous dimension. The enhancement of the radiative mass due to the anomalous dimension $\gamma_m \simeq 1$ was also shown in the context of the modern version of the walking TC based on the Caswell-Banks-Zaks IRFP [15] (see also an earlier work [26] in the context of the one-loop beta function). All these earlier estimates of mass were, however, only rough estimates of the relative enhancement in the generic TC model building, and not the *explicit* estimates for the specific one-family model including the Clebsch-Gordan coefficients as done in the present paper.

In this paper, we compute the mass and the coupling of technipions of a typical walking TC, the Farhi-Susskind one-family model [2], using recent results on a nonperturbative analysis based on the ladder Schwinger-Dyson equation employed in a modern version of walking TC [27]. The masses of technipions charged under the EW gauges are calculated by evaluating one-EW gauge boson exchange diagrams, so that the contributions are cast into the form of integral over the momentum square Q^2 with respect to the difference between vector and axial-vector current correlators ($\Pi_{V\text{-}A}$), similarly to the computation for charged pion mass in QCD. Though those current correlators are quite sensitive to ultraviolet behavior and thus the walking dynamics, it turns out that the EW gauge boson exchange contributions dramatically cancel each other in the ultraviolet region, as was discussed long ago for the naive scale-up version of QCD [9,28,29], so that there arise no sizable corrections to the masses.

The colored technipions, on the other hand, get sizable ultraviolet contributions from the one-gluon exchange diagram, contrary to the charged pions. The size of the corrections without ultraviolet cancellation is actually enhanced by a large logarithmic factor scaled with the ultraviolet scale of TC, $\Lambda_{\rm TC}$, compared to the naive scale-up version of QCD [2]. This is due to the characteristic ultraviolet scaling of $\Pi_{V\text{-}A}$ in the walking TC: the $\Pi_{V\text{-}A}$ in the walking TC damps with the large anomalous dimension $\gamma_m \simeq 1$ more slowly than that in QCD-like dynamics with $\gamma_m \simeq 0$, in such a way that $\Pi_{V\text{-}A} \sim 1/Q^{4-2\gamma_m}$. Thus the amount of integration over the momentum square Q^2 gets larger than that in the case of QCD-like dynamics, depending on the size of the ultraviolet cutoff $\Lambda_{\rm TC}$, as was indicated in Ref. [15].

As in Ref. [2], ETC-induced four-fermion interactions breaking the full chiral $SU(8)_L \times SU(8)_R$ symmetry into the separate chiral symmetries for techniquarks and technileptons give the masses to technipions coupled to the separate chiral currents. The masses also get enhanced due to the chiral condensate enhanced by the large anomalous dimension, as has been expected [3]. Precise estimates of the masses can then be made by using the recent nonperturbative results [27] on the technifermion chiral condensate $\langle \bar{F}F \rangle$ combined with the Pagels-Stokar formula [30] for the technipion decay constant F_π, which allows us to evaluate $\langle \bar{F}F \rangle$ in terms of F_π fixed as $F_\pi = v_{\rm EW}/2 \simeq 123$ GeV. As a result, it turns out that all the technipions are on the order of several hundred GeV (see Table I).

Based on our estimation, we then discuss the phenomenological implications to the LHC signatures focusing on neutral isosinglet technipions in comparison with the SM Higgs.

This paper is organized as follows: In Sec. II we start with a brief review of a low energy effective Lagrangian, which consists of the walking pseudos (technipions and

TABLE I. The technipions and their associated currents and masses in the original one-family model [2]. The masses have been estimated including the enhancement of technifermion condensation in the case of walking TC with $\Lambda_{\rm TC} = 10^3(10^4)$ TeV (see text). Here λ_a ($a = 1, \ldots, 8$) are the Gell-Mann matrices, τ^i $SU(2)$ generators normalized as $\tau^i = \sigma^i/2$ ($i = 1, 2, 3$) with the Pauli matrices σ^i, and the label c attached on the color-triplet technipion field T_c stands for QCD-three colors, $c = r, g, b$.

Technipion	Current	Mass [GeV] (walking TC)
θ_a^i	$\frac{1}{\sqrt{2}}\bar{Q}\gamma_\mu\gamma_5\lambda_a\tau^i Q$	$449(537)\sqrt{\frac{3}{N_{\rm TC}}}$
θ_a	$\frac{1}{2\sqrt{2}}\bar{Q}\gamma_\mu\gamma_5\lambda_a Q$	$449(537)\sqrt{\frac{3}{N_{\rm TC}}}$
T_c^i ($\bar{T}_c^i$)	$\frac{1}{\sqrt{2}}\bar{Q}_c\gamma_\mu\gamma_5\tau^i L$ (H.c.)	$299(358)\sqrt{\frac{3}{N_{\rm TC}}}$
T_c ($\bar{T}_c$)	$\frac{1}{2\sqrt{2}}\bar{Q}_c\gamma_\mu\gamma_5 L$ (H.c.)	$299(358)\sqrt{\frac{3}{N_{\rm TC}}}$
P^i	$\frac{1}{2\sqrt{3}}(\bar{Q}\gamma_\mu\gamma_5\tau^i Q - 3\bar{L}\gamma_\mu\gamma_5\tau^i L)$	502 (ETC)
P^0	$\frac{1}{4\sqrt{3}}(\bar{Q}\gamma_\mu\gamma_5 Q - 3\bar{L}\gamma_\mu\gamma_5 L)$	397 (ETC)

technidilaton) based on nonlinear realization of both chiral and scale symmetries [21–23]. We then explicitly identify the technipion currents coupled to the SM gauge bosons and fermions and couplings necessary to calculate the technipion masses. The walking technipion masses are computed based on the standard current algebra. In Sec. III we address the phenomenological implications to the LHC focusing on neutral isosinglet technipions. Section IV is devoted to summary of this paper. In the Appendix we present a brief discussion about the effects on technidilaton phenomenologies arising from the couplings to the technipions.

II. THE ONE-FAMILY WALKING TECHNIPION MASSES AND COUPLINGS

We begin with an effective Lagrangian relevant to the walking pseudos (technipions and technidilaton) based on the nonlinear realization for both scale and chiral $SU(N_{\rm TF})_L \times SU(N_{\rm TF})_R$ symmetries [21–23]. The building blocks consist of the usual chiral nonlinear base U and technidilaton field ϕ. The U is parametrized as $U = e^{2i\pi/F_\pi}$ where $\pi = \pi^A X^A$ ($A = 1, \ldots, N_{\rm TF}^2 - 1$) with X^A being generators of $SU(N_{\rm TF})$ and F_π denotes the decay constant associated with the spontaneous breaking of the chiral symmetry. The U then transforms under the chiral symmetry as $U \to g_L U g_R^\dagger$ where $g_{L,R} \in SU(N_{\rm TF})_{L,R}$, while under the scale symmetry $\delta U = x^\nu \partial_\nu U$ so does π. The technidilaton field ϕ is, on the other hand, introduced so as to parametrize a nonlinear base for the scale symmetry χ, such that $\chi = e^{\phi/F_\phi}$ with the decay constant for the spontaneous breaking of the scale symmetry F_ϕ. The scale nonlinear base χ then transforms with scale dimension 1, i.e., $\delta\chi = (1 + x^\nu\partial_\nu)\chi$ so that ϕ does nonlinearly as $\delta\phi = F_\phi + x^\nu\partial_\nu\phi$.

One thus constructs the nonlinear Lagrangian [21–23]:

$$\mathcal{L} = \frac{F_\pi^2}{4}\chi^2 {\rm tr}[\mathcal{D}_\mu U^\dagger \mathcal{D}^\mu U] + \mathcal{L}_{\pi ff} + \cdots, \tag{1}$$

where $\mathcal{D}_\mu U$ denotes the covariant derivative acting on U gauged only under the SM $SU(3)_c \times SU(2)_W \times U(1)_Y$ gauge symmetries, which will later be specified to the case of the one-family model. The Yukawa interaction terms between the technipions and SM fermions are included in $\mathcal{L}_{\pi ff}$ which should involve a "spurion field" $S(x)$ [21–23] necessary to reflect the explicit breaking of the scale symmetry due to the dynamical mass generation of the technifermion. Actually, the Yukawa couplings highly depend on modeling of ETC, which arise necessary through the ETC-gauge boson exchanges. We will later discuss the Yukawa couplings to fix the form by considering typical ETC exchange contributions. The ellipses in Eq. (1) include technipion mass terms which are to be studied later.

A. Technipion couplings

In the Farhi-Susskind one-family model [2], the chiral symmetry gets enhanced from the minimal $SU(2)_L \times SU(2)_R$ to $SU(2N_D)_L \times SU(2N_D)_R$, where $N_D = 4$ corresponding to three techniquark Q_c ($c = r, g, b$) and one technilepton (L) doublets. The technifermion condensation $\langle\bar{F}F\rangle \neq 0$ ($F = Q, L$) therefore breaks the enlarged chiral symmetry down to $SU(8)_V$, leading to 63 Nambu-Goldstone bosons in total. The three of them become unphysical to be eaten by W and Z bosons in the same way as in the usual Higgs mechanism, while the other 60 Nambu-Goldstone bosons become pseudos, technipions, to be massive in several ways. The technipions are classified by the isospin and QCD color charges, which are listed in Table I together with the characterized currents coupled to them, where the notation follows the original literature [2].

The technipion couplings in the one-family model are read off from Eq. (1) once the broken generators X^A ($A = 1, \ldots, 63$) that are appropriate to the corresponding broken currents listed in Table I are specified

$$\begin{aligned}\sum_{A=1}^{63}\pi^A(x)X^A &= \sum_{i=1}^{3}\pi^i_{\rm eaten}(x)X^i_{\rm eaten} + \sum_{i=1}^{3}P^i(x)X_P^i + P^0(x)X_P \\ &\quad + \sum_{i=1}^{3}\sum_{a=1}^{8}\theta_a^i(x)X_{\theta a}^i + \sum_{a=1}^{8}\theta_a(x)X_{\theta a} \\ &\quad + \sum_{c=r,g,b}\sum_{i=1}^{3}[T_c^{(1)i}(x)X_{Tc}^{(1)i} + T_c^{(2)i}(x)X_{Tc}^{(2)i}] \\ &\quad + \sum_{c=r,g,b}[T_c^{(1)}(x)X_{Tc}^{(1)} + T_c^{(2)}(x)X_{Tc}^{(2)}],\end{aligned} \tag{2}$$

where

$$
\begin{aligned}
X^i_{\text{eaten}} &= \frac{1}{2}\left(\begin{array}{c|c} \tau^i \otimes 1_{3\times3} & \\ \hline & \tau^i \end{array}\right), \quad X^i_P = \frac{1}{2\sqrt{3}}\left(\begin{array}{c|c} \tau^i \otimes 1_{3\times3} & \\ \hline & -3\cdot\tau^i \end{array}\right), \quad X_P = \frac{1}{4\sqrt{3}}\left(\begin{array}{c|c} 1_{6\times6} & \\ \hline & -3\cdot 1_{2\times2} \end{array}\right), \\
X^i_{\theta a} &= \frac{1}{\sqrt{2}}\left(\begin{array}{c|c} \tau^i \otimes \lambda_a & \\ \hline & 0 \end{array}\right), \quad X_{\theta_a} = \frac{1}{2\sqrt{2}}\left(\begin{array}{c|c} 1_{2\times2} \otimes \lambda_a & \\ \hline & 0 \end{array}\right), \\
X^{(1)i}_{Tc} &= \frac{1}{2}\left(\begin{array}{c|c} & \tau^i \otimes \xi_c \\ \hline \tau^i \otimes \xi_c^\dagger & \end{array}\right), \quad X^{(2)i}_{Tc} = \frac{1}{2}\left(\begin{array}{c|c} & -i\tau^i \otimes \xi_c \\ \hline i\tau^i \otimes \xi_c^\dagger & \end{array}\right), \\
X^{(1)}_{Tc} &= \frac{1}{4}\left(\begin{array}{c|c} & 1_{2\times2} \otimes \xi_c \\ \hline 1_{2\times2} \otimes \xi_c^\dagger & \end{array}\right), \quad X^{(2)}_{Tc} = \frac{1}{4}\left(\begin{array}{c|c} & -i\cdot 1_{2\times2} \otimes \xi_c \\ \hline i\cdot 1_{2\times2} \otimes \xi_c^\dagger & \end{array}\right),
\end{aligned}
\tag{3}
$$

with ξ_c being a three-dimensional unit vector in color space and the generators normalized as $\mathrm{Tr}[X^A X^B] = \delta^{AB}/2$. The color-triplet technipions $\{T^i_c, \bar{T}^i_c\}$ and $\{T_c, \bar{T}_c\}$ are, respectively, constructed from $\{(T^{(1)}_c)^i, (T^{(2)}_c)^i\}$, and $\{T^{(1)}_c, T^{(2)}_c\}$ as

$$
\begin{aligned}
T^i_c &= \frac{(T^{(1)}_c)^i - i(T^{(2)}_c)^i}{\sqrt{2}}, \qquad \bar{T}^i_c = (T^i_c)^\dagger, \\
T_c &= \frac{T^{(1)}_c - iT^{(2)}_c}{\sqrt{2}}, \qquad \bar{T}_c = (T_c)^\dagger.
\end{aligned}
\tag{4}
$$

The covariant derivative $(\mathcal{D}_\mu U)$ in Eq. (1) now reads

$$
\begin{aligned}
\mathcal{D}_\mu U &= \partial_\mu U - i\mathcal{L}_\mu U + iU\mathcal{R}_\mu, \\
\mathcal{L}_\mu &= 2g_W W^i_\mu X^i_{\text{eaten}} + \frac{2}{\sqrt{3}} g_Y B_\mu X_P + \sqrt{2} g_s G^a_\mu X_{\theta_a}, \\
\mathcal{R}_\mu &= 2g_Y B_\mu\left(X^3_{\text{eaten}} + \frac{1}{\sqrt{3}} X_P\right) + \sqrt{2} g_s G^a_\mu X_{\theta_a}.
\end{aligned}
\tag{5}
$$

With this covariant derivative, one can easily see that the $|\mathcal{D}_\mu U|^2$ term in Eq. (1) gives the W boson mass,

$$
m^2_W = \frac{1}{4} g^2_W (4F^2_\pi) = \frac{1}{4} g^2_W v^2_{\text{EW}}, \tag{6}
$$

as well as the Z boson mass, where $v_{\text{EW}} \simeq 246$ GeV.

In order to study the technipion LHC phenomenologies later, we shall next derive the technipion couplings to the SM particles.

1. Couplings to the SM gauge bosons

The technipion couplings to two SM gauge bosons arise from the (covariantized) Wess-Zumino-Witten (WZW) term [31] related to the non-Abelian $SU(8)_L \times SU(8)_R$ anomaly

$$
S_{\text{WZW}}[U, \mathcal{L}, \mathcal{R}], \tag{7}
$$

which includes the couplings as

$$
\begin{aligned}
S_{\text{WZW}}[U, \mathcal{L}, \mathcal{R}] &\ni -\frac{N_{\text{TC}}}{48\pi^2}\int_{M^4} \{\mathrm{tr}[(d\mathcal{L}\mathcal{L} + \mathcal{L}d\mathcal{L})\alpha + (d\mathcal{R}\mathcal{R} + \mathcal{R}d\mathcal{R})\beta] + i\mathrm{tr}[d\mathcal{L}dU\mathcal{R}U^\dagger - d\mathcal{R}dU^\dagger\mathcal{L}U]\} \\
&= -\frac{N_{\text{TC}}}{12\pi^2 F_\pi}\int_{M^4} \mathrm{tr}[(3d\mathcal{V}d\mathcal{V} + d\mathcal{A}d\mathcal{A})\pi + \mathcal{O}(\pi^2)],
\end{aligned}
\tag{8}
$$

where M^4 denote a four-dimensional Minkowski manifold and the things have been written in differential form, and

$$
\alpha = -idUU^\dagger, \qquad \beta = -iU^\dagger dU. \tag{9}
$$

The vector and axial-vector fields $\mathcal{V}$ and $\mathcal{A}$ are expressed in terms of $W^\pm$, Z, photon (A), and gluon (G) fields as follows:

$$
\begin{aligned}
\mathcal{V} &\equiv \frac{\mathcal{R} + \mathcal{L}}{2} = g_s G^a \Lambda^a + eQ_{\text{em}} A + \frac{e}{2sc}(I_3 - 2s^2 Q_{\text{em}})Z + \frac{e}{2\sqrt{2}s}(W^+ I_+ + W^- I_-), \\
\mathcal{A} &\equiv \frac{\mathcal{R} - \mathcal{L}}{2} = -\frac{e}{2sc} I_3 Z - \frac{e}{2\sqrt{2}s}(W^+ I_+ + W^- I_-),
\end{aligned}
\tag{10}
$$

where s ($c^2 = 1 - s^2$) denotes the standard weak mixing angle defined by $g_W = e/s$ and $g_Y = e/c$, and

$$
\begin{aligned}
\Lambda_a &= \sqrt{2} X_{\theta_a}, \qquad I_3 = 2X^3_{\text{eaten}}, \qquad Q_{\text{em}} = I_3 + Y, \\
Y &= \frac{2}{\sqrt{3}} X_P, \qquad I_+ = X^1_{\text{eaten}} + iX^2_{\text{eaten}}, \qquad I_- = (I_+)^\dagger.
\end{aligned}
\tag{11}
$$

Substituting these expressions into the last line of Eq. (8), we find the technipion couplings to two gauge bosons. To the neutral and colorless pion P^0 and color-octet pion θ_a, for instance, we have

$$
\begin{aligned}
S_{P^0gg} &= -\frac{N_{\rm TC}}{16\sqrt{3}\pi^2}\frac{g_s^2}{F_\pi}\int_{M^4} P^0 dG^a dG^a,\\
S_{P^0\gamma\gamma} &= \frac{N_{\rm TC}}{12\sqrt{3}\pi^2}\frac{e^2}{F_\pi}\int_{M^4} P^0 dAdA,\\
S_{P^0Z\gamma} &= \frac{N_{\rm TC}}{6\sqrt{3}\pi^2}\frac{e^2 s}{cF_\pi}\int_{M^4} P^0 dZdA,\\
S_{P^0ZZ} &= \frac{N_{\rm TC}}{12\sqrt{3}\pi^2}\frac{e^2 s^2}{c^2F_\pi}\int_{M^4} P^0 dZdZ,\\
S_{P^0WW} &= 0,
\end{aligned} \tag{12}
$$

and

$$
\begin{aligned}
S_{\theta gg} &= -\frac{N_{\rm TC}}{8\sqrt{2}\pi^2}\frac{g_s^2}{F_\pi}\int_{M^4} d_{abc}\theta^a dG^b dG^c,\\
d_{abc} &\equiv \frac{1}{4}{\rm Tr}[\lambda_a\{\lambda_b,\lambda_c\}],\\
S_{\theta Zg} &= -\frac{N_{\rm TC}}{12\sqrt{2}\pi^2}\frac{g_s e s}{F_\pi c}\int_{M^4}\theta_a dZdG^a,\\
S_{\theta Z\gamma} &= -\frac{N_{\rm TC}}{12\sqrt{2}\pi^2}\frac{g_s e}{F_\pi}\int_{M^4}\theta_a dAdG^a.
\end{aligned} \tag{13}
$$

Note that the P^0-W-W coupling vanishes because the vertex $\propto {\rm tr}[X_P]=0$, which means the cancellation between techniquark and technilepton contributions.

2. Couplings to the SM fermions

As was noted at the beginning of this section, the Yukawa couplings between the technipions and SM fermions depend on models of ETC. We shall here consider a typical ETC embedding the one-family technifermions and SM fermions in a single multiplet. We assume that the ETC carries no SM charges and chiral techniquarks $Q_{L,R}=(U,D)_{L,R}$, and technileptons $L_{L,R}=(N,E)_{L,R}$ are separately included in the ETC multiplets $\mathcal{Q}_{L,R}=\{Q,q\}_{L,R}$ and $\mathcal{L}_{L,R}=\{L,l\}_{L,R}$, along with the SM quarks $q_{L,R}=(q_u,q_d)_{L,R}$ and leptons $l_{L,R}=(\nu,\ell)_{L,R}$. We focus only on flavor-diagonal couplings to avoid the FCNC problem. Then the ETC gauge boson exchanges generically generate the induced four-fermion interactions at the scale $\Lambda_{\rm ETC}$ as

$$
\begin{aligned}
\mathcal{L}^{\rm eff}_{\rm ETC} = -\frac{1}{\Lambda^2_{\rm ETC}}\Big[&\bar{\mathcal{Q}}^i_L\gamma_\mu(T^{\mathcal{Q}})_{ij}\mathcal{Q}^j_L\cdot\bar{\mathcal{Q}}_R\gamma^\mu(T^{\mathcal{Q}})_{kl}\mathcal{Q}^k_R,\\
&+\bar{\mathcal{L}}^i_L\gamma_\mu(T^{\mathcal{L}})_{ij}\mathcal{L}^j_L\cdot\bar{\mathcal{L}}_R\gamma^\mu(T^{\mathcal{L}})_{kl}\mathcal{L}^k_R\Big],
\end{aligned} \tag{14}
$$

where $T^{\mathcal{Q}}$ and $T^{\mathcal{L}}$ denote the ETC generators corresponding to the $\mathcal{Q}$ and $\mathcal{L}$ multiplets, respectively. Performing Fierz rearrangement and picking up only the scalar (S) and pseudoscalar (pS) channels, we are thus left with

$$
\begin{aligned}
\mathcal{L}^{S,pS}_{\rm ETC} = G_{\mathcal{Q}}(\bar{Q}U\bar{q}q_u - \bar{Q}\gamma_5 U\bar{q}\gamma_5 q_u+\cdots)\\
+G_{\mathcal{L}}(\bar{L}E\bar{l}l-\bar{E}\gamma_5 E\bar{l}\gamma_5 l+\cdots),
\end{aligned} \tag{15}
$$

where $G_{\mathcal{Q},\mathcal{L}}\sim 1/\Lambda^2_{\rm ETC}$ which involves all the numerical factors arising from the Fierz transformation on the Dirac spinors, ETC generators $T^{\mathcal{Q}}$ and $T^{\mathcal{L}}$. The first terms in the first and second lines lead to the SM quark and lepton masses through the techniquark and technilepton condensates

$$
m_q = -G_{\mathcal{Q}}\langle\bar{Q}U\rangle, \qquad m_l = -G_{\mathcal{L}}\langle\bar{L}E\rangle. \tag{16}
$$

We next consider the technipion couplings to techniquarks and technileptons. They are completely determined by the low-energy theorem based on the Ward-Takahashi identities for the axial-vector current J^5_μ:

$$
\begin{aligned}
\lim_{q_\mu\to 0} q^\mu\int d^4z e^{iqz}\langle 0|TJ^5_\mu(z)\bar{F}(x)F(0)|0\rangle\\
=\delta_5\langle 0|T\bar{F}(x)F(0)|0\rangle,
\end{aligned} \tag{17}
$$

where $\delta_5\mathcal{O}=[iQ_5,\mathcal{O}]$ denotes the infinitesimal chiral transformation under the chiral charge $Q_5=\int d^3xJ^5_0(x)$ associated with the axial-vector current J^5_μ. The left-hand side is saturated by the technipion pole:

$$
({\rm lhs}) = F_\pi\langle\pi(q=0)|TF(x)\bar{F}(0)|0\rangle, \tag{18}
$$

where the technipion decay constant has been defined as

$$
\langle 0|J^5_\mu(x)|\pi(q)\rangle = -iF_\pi q_\mu e^{-iqx}. \tag{19}
$$

Taking the Fourier transform of Eq. (17) with respect to p, we find the amputated Yukawa vertex function $\chi_{\pi FF}(0,p)$:

$$
\begin{aligned}
\chi_{\pi FF}(0,p) &\equiv S_F^{-1}(p)\cdot\langle\pi(q=0)|TF(x)\bar{F}(0)|0\rangle\cdot S_F^{-1}(p)\\
&= S_F^{-1}(p)\cdot\left(\frac{1}{F_\pi}\delta_5 S_F(p)\right)\cdot S_F^{-1}(p)\\
&= -\frac{1}{F_\pi}\delta_5 S_F^{-1}(p),
\end{aligned} \tag{20}
$$

with $S_F(p)$ being the (full) F-fermion propagator.

To be concrete, consider the P^0 technipion. Then the chiral transformations for the techniquark and technileptons are read off from Table I as $\delta_{P^0}Q(x)=-\frac{i}{4\sqrt{3}}\gamma_5 Q(x)$ and $\delta_{P^0}L(x)=\frac{3i}{4\sqrt{3}}\gamma_5 L(x)$, so that

$$
\begin{aligned}
\delta_{P^0}S_Q^{-1}(p) &= -\frac{1}{4\sqrt{3}}i\{\gamma_5,S_Q^{-1}(p)\}\\
&= -\frac{1}{2\sqrt{3}}i\gamma_5\Sigma_Q(p^2)\cdot Z_Q(p^2),\\
\delta_{P^0}S_L^{-1}(p) &= \frac{3}{4\sqrt{3}}i\{\gamma_5,S_L^{-1}(p)\}\\
&= \frac{3}{2\sqrt{3}}i\gamma_5\Sigma_L(p^2)\cdot Z_L(p^2),
\end{aligned} \tag{21}
$$

where we have parametrized the F-fermion propagator as $S_F(p)=[iZ_F(p^2)(\Sigma_F(p^2)-\not{p})]^{-1}$ with the mass function

$\Sigma_F(p^2)$ and wave function renormalization $Z_F(p^2)$. Putting Eq. (21) into Eq. (20) and defining the renormalized Yukawa vertex function as

$$\chi^R_{P^0FF}(0,p) \equiv Z_F^{-1}(p^2)\chi_{P^0FF}(0,p), \tag{22}$$

we thus find

$$\begin{aligned}\chi^R_{P^0QQ}(0,p) &= \frac{i}{2\sqrt{3}}\frac{\gamma_5\Sigma_Q(p^2)}{F_\pi},\\ \chi^R_{P^0LL}(0,p) &= -\frac{3i}{2\sqrt{3}}\frac{\gamma_5\Sigma_L(p^2)}{F_\pi}.\end{aligned} \tag{23}$$

Now that we have obtained the Yukawa vertex functions in Eq. (23) and specified the ETC-induced four-fermion terms in Eq. (15), it is straightforward to calculate the technipion (P^0) Yukawa coupling to the SM quarks and leptons just by evaluating the following amplitude (see Fig. 1):

$$\begin{aligned}&i\mathcal{M}(P^0(0), f(p), f(p))\\ &\quad = -C_f\cdot\frac{iG_{Q,\mathcal{L}}}{2\sqrt{3}F_\pi}\,\mathrm{Tr}\int\frac{d^4k}{(2\pi)^4}\\ &\qquad\times[S_F^R(k)\gamma_5 S_F^R(k)\gamma_5\Sigma(k^2)]\cdot\bar{u}_f(p)\gamma_5 u_f(p),\end{aligned} \tag{24}$$

where $C_f = (1,-3)$ for $f=(q,l)$, $u_f(p)$ is the wave function of f fermion, and $S_F^R(p)$ is the renormalized propagator for the F fermion defined as $S_F^R(p) = [i(\Sigma_F(p^2) - \not{p})]^{-1}$. This amplitude is rewritten as

$$\begin{aligned}&i\mathcal{M}(P^0(0), f(p), f(p))\\ &\quad = -C_f\cdot\frac{G_{Q,\mathcal{L}}}{2\sqrt{3}F_\pi}\,\mathrm{Tr}\int\frac{d^4k}{(2\pi)^4}[S_F^R(k)]\cdot\bar{u}_f(p)\gamma_5 u_f(p)\\ &\quad = C_f\cdot\frac{G_{Q,\mathcal{L}}}{2\sqrt{3}F_\pi}\cdot\langle\bar{F}F\rangle\cdot\bar{u}_f(p)\gamma_5 u_f(p).\end{aligned} \tag{25}$$

Noting Eq. (16), we find

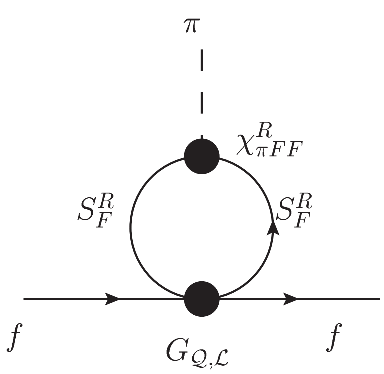

FIG. 1. The diagram yielding the technipion Yukawa vertex amplitude to the SM quarks and leptons such as Eq. (24), involving the ETC-induced four-fermion vertices in Eq. (15) and the technipion Yukawa vertices to the SM fermions in Eq. (23).

$$\begin{aligned}i\mathcal{M}(P^0, q(p), q(p)) &= \frac{m_q}{2\sqrt{3}F_\pi}\cdot\bar{u}_q(p)\gamma_5 u_q(p),\\ i\mathcal{M}(P^0, l(p), l(p)) &= -\frac{3m_l}{2\sqrt{3}F_\pi}\cdot\bar{u}_l(p)\gamma_5 u_l(p).\end{aligned} \tag{26}$$

These matrix elements imply the Yukawa coupling terms:

$$\mathcal{L}_{P^0ff} = -\frac{i}{2\sqrt{3}F_\pi}P^0\Big[\sum_q m_q\bar{q}\gamma_5 q - 3\sum_l m_l\bar{l}\gamma_5 l\Big]. \tag{27}$$

One can easily derive similar formulas for other technipions. For instance, it turns out that the θ_a-f-f coupling takes the form[5]

$$\mathcal{L}_{\theta ff} = -\frac{\sqrt{2}i}{F_\pi}\theta_a\Big[\sum_q m_q\bar{q}\gamma_5\Big(\frac{\lambda_a}{2}\Big)q\Big]. \tag{28}$$

B. Technipion masses

In this subsection we shall calculate the technipion masses in the one-family model embedded in the walking TC. The masses of technipions arise as explicit breaking effects of the full chiral $SU(8)_L\times SU(8)_R$ symmetry associated with the chiral transformation yielding the chiral currents as listed in Table I. There are two sources giving such explicit breaking effects: one is from the SM gauge interactions, while the other from ETC-induced four-fermion interactions.

1. Electroweak-origin mass

The EW radiative corrections give rise to masses for the charged technipions $\pi^\pm = \{\theta_a^\pm, T_c^\pm(\bar{T}_c^\pm), P^\pm\}$ analogously to electromagnetic corrections to the charged pion mass in QCD. The charged pion mass-squared $\Delta m^2_{\pi^\pm}$ can be estimated by taking into account one-photon and Z boson exchanges as illustrated in Fig. 2:

$$\begin{aligned}\Delta m^2_{\pi^\pm} &= (\Delta m^2_{\pi^\pm})_\gamma + (\Delta m^2_{\pi^\pm})_Z,\\ (\Delta m^2_{\pi^\pm})_\gamma &= -\frac{i}{2}e^2\int d^4x D^{(\gamma)}_{\mu\nu}(x)\langle\pi^+|TJ^\mu_{\rm em}(x)J^\nu_{\rm em}(0)|\pi^+\rangle,\\ (\Delta m^2_{\pi^\pm})_Z &= -\frac{i}{2}\frac{e^2}{4s^2c^2}\int d^4x D^{(Z)}_{\mu\nu}(x)\langle\pi^+|TJ^\mu_Z(x)J^\nu_Z(0)|\pi^+\rangle,\end{aligned} \tag{29}$$

where $D^{(\gamma,Z)}_{\mu\nu}$ denote the photon and Z boson propagators, $s^2(=1-c^2)$ stands for the usual weak mixing angle, and $J^\mu_{{\rm em},Z}$ are the electromagnetic and Z boson currents composed of technifermions (Q_c, L) defined by

[5]A set of more general Yukawa coupling terms was discussed in Ref. [32].

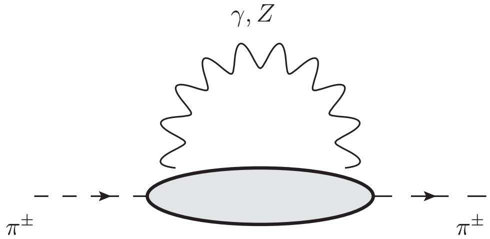

FIG. 2. The one-photon and Z boson exchange graphs contributing to the masses of the electrically charged pions $\pi^\pm = \{\theta_a^\pm, T_c^\pm(\bar{T}_c^\pm), P^\pm\}$.

$$\mathcal{L}_{\gamma FF,ZFF} = eJ^\mu_{\rm em}A_\mu + \frac{e}{2sc}J^\mu_Z Z_\mu,$$
$$J^\mu_{\rm em} = \bar{Q}_c\gamma^\mu\begin{pmatrix}2/3 & 0\\ 0 & -1/3\end{pmatrix}Q_c + \bar{L}\gamma^\mu\begin{pmatrix}0 & 0\\ 0 & -1\end{pmatrix}L,$$
$$J^\mu_Z = (c^2 - s^2)\{\bar{Q}_c\gamma^\mu\tau^3 Q_c + \bar{L}\gamma^\mu\tau^3 L\} - 2s^2\left\{\frac{1}{6}\bar{Q}_c\gamma^\mu Q_c - \frac{1}{2}\bar{L}\gamma^\mu L\right\} - \{\bar{Q}_c\gamma^\mu\gamma_5\tau^3 Q_c + \bar{L}\gamma^\mu\gamma_5\tau^3 L\}. \quad (30)$$

By using the reduction formula together with the partially conserved axial-vector current (PCAC), $\partial_\mu J^\mu_{\pi^\pm}(x) = \sqrt{2}F_\pi m_\pi^2\pi^\pm(x)$, the current algebra technique allows us to rewrite Eq. (29) in terms of the vector and axial-vector current correlators.

To the colorless electrically charged technipions $P^\pm$ coupled to the associated currents $J^\mu_{P^\pm} = \frac{1}{2\sqrt{3}}\times[\bar{Q}_c\gamma^\mu\gamma_5\tau^\pm Q_c - 3\bar{L}\gamma^\mu\gamma_5\tau^\pm L]$, we find

$$(\Delta m^2_{P^\pm})_\gamma = \frac{\alpha_{\rm EM}}{16\pi F_\pi^2}\int_0^\infty dQ^2[\Pi^Q_{V\text{-}A}(Q^2) + 9\Pi^L_{V\text{-}A}(Q^2)],$$
$$(\Delta m^2_{P^\pm})_Z = -\frac{\alpha_{\rm EM}}{16\pi F_\pi^2}\int_0^\infty \frac{dQ^2 Q^2}{m_Z^2 + Q^2}[\Pi^Q_{V\text{-}A}(Q^2) + 9\Pi^L_{V\text{-}A}(Q^2)], \quad (31)$$

where $\alpha_{\rm EM} = e^2/(4\pi)$ and $Q^2 = -p^2$ denotes Euclidean momentum squared, and $\Pi^F_{V\text{-}A}(Q^2) \equiv \Pi^F_V(Q^2) - \Pi^F_A(Q^2)$ $(F = Q_c, L)$ with $\Pi^F_{V(A)}$ is the vector (axial-vector) current correlator defined as

$$i\int d^4x e^{-ipx}\langle 0|T(\bar{F}(x)\gamma^\mu\tau^a F(x)\bar{F}(0)\gamma^\nu\tau^b F(0))|0\rangle = \left(\frac{p^\mu p^\nu}{p^2} - g^{\mu\nu}\right)\delta^{ab}\Pi^F_V(Q^2), \quad (32)$$

$$i\int d^4x e^{-ipx}\langle 0|T(\bar{F}(x)\gamma^\mu\gamma_5\tau^a F(x)\bar{F}(0)\gamma^\nu\gamma_5\tau^b F(0))|0\rangle = \left(\frac{p^\mu p^\nu}{p^2} - g^{\mu\nu}\right)\delta^{ab}\Pi^F_A(Q^2). \quad (33)$$

Note the relative sign between the photon and Z boson contributions in Eq. (31), which give the dramatic cancellation in a way similar to the collective symmetry breaking in the little Higgs, such that the total contribution becomes

$$\Delta m^2_{P^\pm} = \frac{\alpha_{\rm EM}}{16\pi F_\pi^2}\int_0^\infty dQ^2\frac{m_Z^2}{m_Z^2 + Q^2}[\Pi^Q_{V\text{-}A}(Q^2) + 9\Pi^L_{V\text{-}A}(Q^2)]. \quad (34)$$

It is easy to derive similar formulas for the other charged technipions as well.

The right-hand side of Eq. (34) can be split into two terms:

$$\int_0^\infty dQ^2\frac{m_Z^2}{m_Z^2 + Q^2}\Pi^F_{V\text{-}A}(Q^2) = \int_0^{\Lambda_\chi^2} dQ^2\frac{m_Z^2}{m_Z^2 + Q^2}\Pi^F_{V\text{-}A}(Q^2) + \int_{\Lambda_\chi^2}^{\Lambda^2_{\rm TC}(\to\infty)} dQ^2\frac{m_Z^2}{m_Z^2 + Q^2}\Pi^F_{V\text{-}A}(Q^2), \quad (35)$$

where $\Lambda_\chi \simeq \frac{4\pi F_\pi}{\sqrt{N_{\rm TF}}}$ [6] above which scale $(Q^2 > \Lambda_\chi^2)$ the operator product expansion for $\Pi^F_{V,A}(Q^2)$ is assumed to be valid. The contributions in the infrared region $(Q^2 < \Lambda_\chi^2)$ can be computed using the current algebra [9] or chiral perturbation [28,29], so that the first term in Eq. (35) yields

$$(\Delta m^2_{P^\pm})_{Q^2<\Lambda_\chi^2} = \frac{3\alpha_{\rm EM}}{4\pi}m_Z^2\log\frac{\Lambda_\chi^2}{m_Z^2} \simeq (9\ {\rm GeV})^2, \quad (36)$$

for $F_\pi = 123$ GeV. On the other hand, for the ultraviolet region $(Q^2 > \Lambda_\chi^2)$ we may use the operator product expansion

$$\Pi^F_{V\text{-}A}(Q^2) \underset{Q^2>\Lambda_\chi^2}{\simeq} \frac{4(N_{\rm TC}^2 - 1)}{N_{\rm TC}^2}\left(\frac{Q^2}{\mu^2}\right)^{\gamma_m}\frac{\alpha(\mu)\langle\bar{F}F\rangle^2_\mu}{Q^4} \quad (37)$$

with a renormalization scale μ. Note that only relevant operators to the technipion mass are chiral symmetry breaking operators enhanced by the large mass anomalous dimension $\gamma_m \sim 1$, which are actually dominated by $\langle\bar{F}F\rangle^2$, with other operators being not enhanced comparable to $\langle\bar{F}F\rangle^2$. Although the OPE is not quite accurate near the infrared region $Q \simeq \Lambda_\chi$, such an ambiguity gives only a small portion compared with the effects considered here and hence does not affect our conclusion. Taking into account $\langle\bar{L}L\rangle = 1/3\langle\bar{Q}Q\rangle$ and letting $\langle\bar{L}L\rangle$ be $\langle\bar{F}F\rangle$, we thus find

[6] For the presence of the number of fermions in the chiral symmetry breaking scale Λ_χ, see Ref. [33].

$$\int_{\Lambda_\chi^2}^{\Lambda_{\rm TC}^2(\to\infty)} dQ^2 \frac{m_Z^2}{m_Z^2+Q^2}[\Pi_{V\text{-}A}^{Q}(Q^2)+9\Pi_{V\text{-}A}^{L}(Q^2)] \simeq \frac{48\pi\langle\bar{F}F\rangle_{\Lambda_\chi}^2}{N_{\rm TC}\Lambda_\chi^2}\log\left(1+\frac{m_Z^2}{\Lambda_\chi^2}\right), \tag{38}$$

where we used $\alpha \simeq \alpha_c = \pi/3(C_2(F)) = \frac{2\pi N_{\rm TC}}{3(N_{\rm TC}^2-1)}$ [27].

In order to make the right-hand side of Eq. (38) more explicit, we shall evaluate the chiral condensate $\langle\bar{F}F\rangle$,

$$\langle\bar{F}F\rangle_{\Lambda_{\rm TC}} = -\frac{N_{\rm TC}}{4\pi^2}m_F^3\int_0^{\Lambda_{\rm TC}^2/m_F^2\to\infty} dx\frac{x\Sigma(x)}{x+\Sigma^2(x)}, \tag{39}$$

where $\Sigma(x)=\Sigma(-p^2)/m_F$ denotes the mass function of technifermion normalized as $\Sigma(1)=1$. At the dynamical technifermion mass scale m_F, the chiral condensate may be defined as

$$\langle\bar{F}F\rangle_{m_F} \equiv -\kappa_c\frac{N_{\rm TC}}{4\pi^2}m_F^3, \tag{40}$$

where κ_c is an overall coefficient to be determined once the nonperturbative calculation is done. Using the scaling law

$$\langle\bar{F}F\rangle_{\Lambda_{\rm TC}} \simeq \left(\frac{\Lambda_{\rm TC}}{\mu}\right)^{\gamma_m}\langle\bar{F}F\rangle_\mu, \qquad \gamma_m \simeq 1. \tag{41}$$

Note that the dynamical mass m_F can in general be related to the technipion decay constant F_π as

$$F_\pi^2 \equiv \kappa_F^2\frac{N_{\rm TC}}{4\pi^2}m_F^2, \tag{42}$$

with the overall coefficient κ_F to be fixed by the straightforward calculation. Using Eqs. (40) and (42) together with Eq. (41), we thus express the chiral condensate renormalized at Λ_χ in terms of F_π:

$$\langle\bar{F}F\rangle_{\Lambda_\chi} = -\left(\frac{\kappa_c}{\kappa_F^2}\right)\Lambda_\chi F_\pi^2. \tag{43}$$

Putting Eq. (43) into Eq. (38) and taking into account Eq. (36), we arrive at a concise formula,

$$\Delta m_{P^\pm}^2 \simeq \frac{3\alpha_{\rm EM}(\Lambda_\chi)}{4\pi}m_Z^2\log\frac{\Lambda_\chi^2}{m_Z^2}+\frac{3\alpha_{\rm EM}(\Lambda_\chi)}{N_{\rm TC}} \times\left(\frac{\kappa_c}{\kappa_F^2}\right)^2F_\pi^2\log\left(1+\frac{m_Z^2}{\Lambda_\chi^2}\right). \tag{44}$$

Note that the second term from the ultraviolet region ($Q^2>\Lambda_\chi^2$) is almost negligible since $(m_Z/\Lambda_\chi)^2\sim 10^{-3}\times N_{\rm TF}$. Thus the EW corrections to the charged technipion mass in the walking TC are dominated by the infrared contributions of order of a few GeV [Eq. (36)], to be negligible compared to another source from ETC as will be discussed later.

2. QCD-origin mass

The QCD-gluon exchanges give masses to the colored technipions, θ_a^i, θ_a, and T_c^i ($\bar{T}_c^i$). Those corrections can be estimated in a way similar to the photon contribution to the charged pion mass discussed above, simply by scaling $(\Delta m_{\pi^\pm}^2)_\gamma$ in Eq. (29):

$$\frac{\Delta m_{3,8}^2}{(\Delta m_{\pi^\pm}^2)_\gamma} = C_2(R)\frac{\alpha_s(\Lambda_\chi)}{\alpha_{\rm EM}(\Lambda_\chi)}, \tag{45}$$

where $C_2(R)=\frac{4}{3}(3)$ for color triplets (octets). The photon exchange contribution $(\Delta m_{\pi^\pm}^2)_\gamma$ is decomposed into two parts—infrared and ultraviolet terms—in the same way as done in Eq. (35). The ultraviolet term then turns out to be highly dominant due to the large logarithmic enhancement coming from the slow damping behavior of $\Pi_{V\text{-}A}(Q^2)$ in the walking TC, $\Pi_{V\text{-}A}^F(Q^2)\sim\langle\bar{F}F\rangle^2/Q^2$ [See Eq. (37)]:

$$(\Delta m_{\pi^\pm}^2)_\gamma \simeq \frac{9\alpha_{\rm EM}}{8\pi F_\pi^2}\int_{\Lambda_\chi^2}^{\Lambda_{\rm TC}^2(\to\infty)}\Pi_{V\text{-}A}^F(Q^2) \simeq \frac{3\alpha_{\rm EM}}{N_{\rm TC}}\left(\frac{\kappa_c}{\kappa_F^2}\right)^2F_\pi^2\log\frac{\Lambda_{\rm TC}^2}{\Lambda_\chi^2}, \tag{46}$$

where we used Eq. (43) and put $\alpha(\Lambda_\chi)=\alpha_c=\pi/(3C_2(F))$. The colored technipion masses are thus estimated for triplets and octets as follows:

$$\Delta m_3 \simeq 299(358)\ {\rm GeV}\sqrt{\frac{3}{N_{\rm TC}}\left(\frac{\kappa_c}{4.0}\right)\left(\frac{1.4}{\kappa_F}\right)^2}, \quad \Delta m_8 \simeq 449(537)\ {\rm GeV}\sqrt{\frac{3}{N_{\rm TC}}\left(\frac{\kappa_c}{4.0}\right)\left(\frac{1.4}{\kappa_F}\right)^2}, \tag{47}$$

for $\Lambda_{\rm TC}\simeq 10^3(10^4)$ TeV. Here we have used $\alpha_s(\Lambda_\chi)\simeq 0.1$, $F_\pi=123$ GeV, and taken the values of κ_c and κ_F from the recent result based on the ladder Schwinger-Dyson analysis [27].

The estimated numbers in Eq. (47) are compared with those based on a naive scale-up version of QCD [2], which are obtained by replacing $(\Delta m_{\pi^\pm}^2)_\gamma$ with $(\Delta m_{\pi^\pm}^2)_{\rm QCD}\simeq(35\ {\rm MeV})^2$ and supplying the scaling factor $(F_\pi/f_\pi)^2\simeq(1323)^2$ in the right-hand side of Eq. (45):

$$\text{QCD scale-up: } \Delta m_3 \simeq 193\ {\rm GeV}\sqrt{\frac{3}{N_{\rm TC}}}, \quad \Delta m_8 \simeq 290\ {\rm GeV}\sqrt{\frac{3}{N_{\rm TC}}}. \tag{48}$$

This implies that the masses are enhanced by about 50% (85%) for $\Lambda_{\rm TC}=10^3(10^4)$ TeV due to the walking dynamics yielding the slow damping behavior of $\Pi_{V\text{-}A}(Q^2)$ in the high momentum region, in accord with a recent discussion in Ref. [15] and an earlier work [26].

3. ETC-origin mass

The technipions $P^{i,0}$ ($i = 1, 2, 3$) associated with the currents generated by the separate chiral rotations between techniquarks and technileptons may acquire the masses by ETC-induced four-fermion interactions as in Eq. (15),

$$\mathcal{L}^{\rm ETC}_{\text{4-fermi}}(\Lambda_{\rm ETC}) = \frac{1}{\Lambda^2_{\rm ETC}}[\bar{Q}Q\bar{L}L - \bar{Q}\gamma_5\sigma^a Q\bar{L}\gamma_5\sigma^a L], \quad (49)$$

which is SM gauge invariant but breaks the full chiral symmetry into the separate chiral symmetries associated with the techniquarks and technileptons. The masses are then calculated in a way similar to the gauge boson exchange contributions to the charged pion masses in Eq. (29) with use of the reduction formula, current algebra, and associated PCAC relations $\partial_\mu J^\mu_{P^{i,0}}(x) = F_\pi m_P^2 P^{i,0}(x)$:

$$\begin{aligned}(\Delta m^2_{P^{i,0}})_{\rm ETC} &= -\langle P^{i,0}|\mathcal{L}^{\rm ETC}_{\text{4-fermi}}(\Lambda_{\rm ETC})|P^{i,0}\rangle \\ &= \frac{1}{F_\pi^2}\langle 0|[\mathbf{Q}_{P^{i,0}},[\mathbf{Q}_{P^{i,0}},\mathcal{L}^{\rm ETC}_{\text{4-fermi}}(\Lambda_{\rm ETC})]]|0\rangle, \quad (50)\end{aligned}$$

where $\mathbf{Q}_{P^{i,0}}$ denote the chiral charges defined as $\mathbf{Q}_{P^{i,0}} = \int d^3x J^0_{P^{i,0}}(x)$. For each technipion, we thus find

$$\begin{aligned}(\Delta m^2_{P^0})_{\rm ETC} &= \frac{40}{48}\frac{\langle 0|(\bar{Q}Q\bar{L}L)_{\Lambda_{\rm ETC}}|0\rangle}{F_\pi^2\Lambda^2_{\rm ETC}} = \frac{5}{2}\frac{\langle 0|(\bar{F}F)_{\Lambda_{\rm ETC}}|0\rangle^2}{F_\pi^2\Lambda^2_{\rm ETC}}, \\ (\Delta m^2_{P^i})_{\rm ETC} &= \frac{16}{12}\frac{\langle 0|(\bar{Q}Q\bar{L}L)_{\Lambda_{\rm ETC}}|0\rangle}{F_\pi^2\Lambda^2_{\rm ETC}} = 4\frac{\langle 0|(\bar{F}F)_{\Lambda_{\rm ETC}}|0\rangle^2}{F_\pi^2\Lambda^2_{\rm ETC}}. \end{aligned} \quad (51)$$

Using Eqs. (41) and (43), we arrive at

$$\begin{aligned}\Delta m^{\rm ETC}_{P^0} &= \sqrt{\frac{5}{2}}\left(\frac{\kappa_c}{\kappa_F^2}\right)F_\pi \simeq 397\ {\rm GeV}\left(\frac{\kappa_c}{4.0}\right)\left(\frac{1.4}{\kappa_F}\right)^2, \\ \Delta m^{\rm ETC}_{P^i} &= 2\left(\frac{\kappa_c}{\kappa_F^2}\right)F_\pi \simeq 502\ {\rm GeV}\left(\frac{\kappa_c}{4.0}\right)\left(\frac{1.4}{\kappa_F}\right)^2,\end{aligned} \quad (52)$$

where in the last expressions we have quoted the values of κ_c and κ_F from Ref. [27]. It is remarkable to note that since the $P^\pm$ mass becomes larger than the top quark mass, the current experimental limits on charged Higgs bosons [34] are inapplicable to the walking $P^\pm$, where the limits are set based on the top quark decays to the charged Higgs. A new proposal to constrain the walking $P^\pm$ is to be explored in the future.

It is noted that in this paper we totally disregard a possible mixing between P^0 and P^3 due to the isospin (custodial symmetry) breaking effects, which are higher order effects (for the pure TC sector) coming from the operator in Eq. (15) in the ETC framework needed to reproduce the realistic mass of the SM fermions, in particular the top and bottom mass splitting. For the moment there exists no realistic concrete ETC mechanism to produce such a mass splitting without conflict with the T parameter constraint, and hence it is premature to evaluate the mixing effects. More detailed analysis will be dealt with in future investigations.

To summarize, all the estimated masses that have been discussed so far are displayed in Table I.

III. THE LHC SIGNATURES OF ONE-FAMILY WALKING TECHNIPIONS

In this section we shall discuss the LHC signatures of the one-family walking technipions, especially focusing on neutral isosinglet scalars (P^0 and θ_a) in comparison with the SM Higgs.

A. Isosinglet-colorless technipion P^0

From Eq. (12) we compute the P^0 decay widths to the SM gauge boson pairs to get

$$\begin{aligned}\Gamma(P^0 \to gg) &= \frac{N^2_{\rm TC}\alpha_s^2 G_F m^3_{P^0}}{12\sqrt{2}\pi^3}, \\ \Gamma(P^0 \to \gamma\gamma) &= \frac{N^2_{\rm TC}\alpha^2_{\rm EM} G_F m^3_{P^0}}{54\sqrt{2}\pi^3}, \\ \Gamma(P^0 \to Z\gamma) &= \frac{N^2_{\rm TC}\alpha^2_{\rm EM} G_F m^3_{P^0}s^2}{27\sqrt{2}\pi^3 c^2}\left(1 - \frac{m_Z^2}{m^2_{P_0}}\right)^3, \\ \Gamma(P^0 \to ZZ) &= \frac{N^2_{\rm TC}\alpha^2_{\rm EM} G_F m^3_{P^0}s^4}{54\sqrt{2}\pi^3 c^4}\left(1 - \frac{4m_Z^2}{m^2_{P_0}}\right)^{3/2}, \\ \Gamma(P^0 \to WW) &= 0,\end{aligned} \quad (53)$$

where use has been made of $F_\pi = v_{\rm EW}/2$ and $1/v^2_{\rm EW} = \sqrt{2}G_F$ with G_F being the Fermi constant. Similarly from Eq. (27), we also calculate the decay rates to the SM fermion pairs to find

$$\Gamma(P^0 \to f\bar{f}) = A_f \cdot \frac{G_F m_{P^0} m_f^2}{4\sqrt{2}\pi}\left(1 - \frac{4m_f^2}{m^2_{P^0}}\right)^{1/2}, \quad (54)$$

where $A_f = 1(3)$ for quarks (leptons). The P^0 decay properties are summarized in Table II.

TABLE II. The P^0 total width, relevant branching fraction, and numbers regarding the LHC signatures at 397 GeV. Here we have defined $r_{\rm GF} \equiv \sigma^{P^0}_{\rm GF}/\sigma^{h_{\rm SM}}_{\rm GF}$ with the gluon fusion production cross section at $\sqrt{s} = 7$ TeV $\sigma_{\rm GF}$, $r^X_{\rm BR} \equiv {\rm BR}(P^0 \to X)/{\rm BR}(h_{\rm SM} \to X)$, $R_X \equiv r_{\rm GF} \times r^X_{\rm BR}$. The branching ratios and 7 TeV LHC production cross section for the SM Higgs are taken from Ref. [36].

$N_{\rm TC}$	$\Gamma^{P^0}_{\rm tot}$ [GeV]	${\rm BR}_{gg}$	${\rm BR}_{\tau^+\tau^-}$	${\rm BR}_{t\bar{t}}$		
3	4.0	4.3×10^{-2}	6.1×10^{-4}	9.5×10^{-1}		
4	4.2	7.4×10^{-2}	5.9×10^{-4}	9.2×10^{-1}		
	$r_{\rm GF}$	$r^{gg}_{\rm BR}$	$r^{\tau^+\tau^-}_{\rm BR}$	$r^{t\bar{t}}_{\rm BR}$	$R_{\tau^+\tau^-}$	$R_{t\bar{t}}$
3	5.0	35	21	6.5	96	30
4	9.0	60	20	6.3	165	52

Of interest is that the P^0 decays to W and Z boson pairs are highly suppressed, as was noted in Ref. [25], due to the techniquark and lepton cancellation in loops. The P^0 is thus almost completely gaugephobic to be definitely distinguishable from the SM Higgs at the LHC. Besides the obvious WW mode, one can indeed check the gaugephobicity also to the ZZ mode by evaluating a ratio of the $P^0 \to ZZ$ decay width to the corresponding quantity of the SM Higgs which roughly scales like

$$\frac{\Gamma(P^0 \to ZZ)}{\Gamma(h_{\rm SM} \to ZZ)} \approx \left(\frac{N_{\rm TC}}{3}\right)^2 \left(\frac{\sqrt{2}\alpha_{\rm EM}}{\sqrt{3}\pi}\frac{s^2}{c^2}\right)^2 \sim 10^{-7} \times \left(\frac{N_{\rm TC}}{3}\right)^2. \tag{55}$$

Thus the P^0 signals through decays to the weak gauge bosons are to be almost invisible at the LHC.

On the other hand, the P^0 decays to fermion pairs get enhanced since the gluon fusion (GF) production cross section is highly enhanced (by about a factor of 10) due to technifermion loop contributions:

$$\frac{\sigma(gg \to P^0)}{\sigma(gg \to h_{\rm SM})} \approx 7\left(\frac{N_{\rm TC}}{3}\right)^2, \tag{56}$$

where the heavy quark mass limit for top and bottom quarks has been taken. Accordingly, the cross section times branching ratio for decays to the light fermion pairs are also enhanced compared to those of the SM Higgs. In fact, the current LHC data on the $\tau^+\tau^-$ channel severely constrain the P^0 mass to exclude it up to $m_{P^0} = 2m_t$ [25]. However, note that as shown in the previous section, the typical value of m_{P^0} estimated in the walking TC exceeds the top pair threshold, i.e., $m_{P^0} = 397$ GeV (see Table I). In such a higher mass region $m_{P^0} \geq 2m_t$, the cross section $\sigma(pp \to P^0 \to \tau^+\tau^-)$ gets highly suppressed to be about order of 10^{-2} pb at around 397 GeV [25], which is well below the current 95% C.L. upper bound $\sim$1 pb at around 397 GeV [35]. This is because the $t\bar{t}$ channel is open to be dominant (see Fig. 3).

In Ref. [25], the analysis has been done with simple-minded Yukawa couplings for the technipions assumed, namely, setting the overall factors associated with the pion currents, like $(1/2\sqrt{3}, 3/2\sqrt{3})$ for the couplings (g_{P^0qq}, g_{P^0ll}) in Eq. (27), to unity. The present study has properly incorporated such factors specific to the one-family technipions, so that the current LHC limit from the $\tau^+\tau^-$ channel gets slightly modified as seen from Fig. 3 to allow a small window below $2m_t$.

The branching fraction of P^0 with $m_{P^0} = 397$ GeV is indeed governed by the $t\bar{t}$ mode, which is about 99% compared to the SM Higgs case at around 397 GeV $\mathrm{BR}_{t\bar{t}}^{h_{\rm SM}} \simeq 15\%$ [36], but the total width remains as small

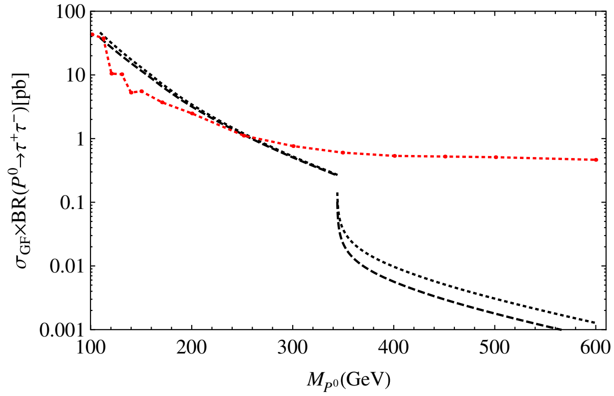

FIG. 3 (color online). The cross section $\sigma_{\rm GF}(pp \to P^0)$ times branching ratio $\mathrm{BR}(P^0 \to \tau^+\tau^-)$ as a function of the P^0 mass in a high mass range up to 600 GeV for $N_{\rm TC} = 3$ (dashed black) and 4 (dotted black) at the 7 TeV LHC, in units of pb. The red dotted line stands for the current 95% C.L. upper bound from the ATLAS experiments with 1.06 fb^{-1} [35].

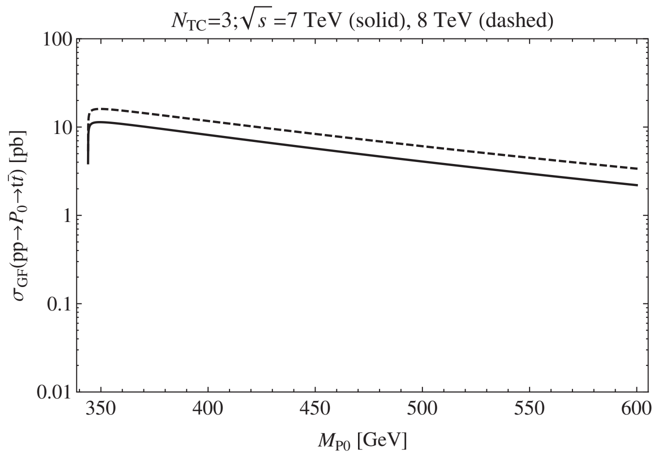

FIG. 4. The P^0 contribution to the $t\bar{t}$ total cross section as a function of the P^0 mass for $N_{\rm TC} = 3$ at $\sqrt{s} = 7$ TeV (solid) and 8 TeV (dashed), in units of pb.

as a few GeV, so it is still a narrow resonance. Thus the P^0 peak in the highly enhanced $t\bar{t}$ channel will be distinct to be measured by the $t\bar{t}$ invariant mass distribution [37]. Figure 4 shows the P^0 contribution to the $t\bar{t}$ total cross section in the narrow width approximation as a function of the P^0 mass in a range above $2m_t$. The P^0 resonance effect thus will yield about 8 pb to the $t\bar{t}$ total cross section at the mass $m_{P^0} = 397$ GeV, which is still within the current 1 sigma error of the $\sigma_{t\bar{t}}$ measurement at the LHC [38], and hence will be tested more clearly by the upcoming 2012 data.

B. Isosinglet-color octet technipion θ_a

From Eqs. (13) and (28), the θ_a decay widths to the SM gauge boson and fermion pairs are calculated to be

TABLE III. The θ_a total width, relevant branching fraction, and numbers regarding the LHC signatures. Here we have defined $r_{\rm GF} \equiv \sigma_{\rm GF}^{\theta_a}/\sigma_{\rm GF}^{h_{\rm SM}}$ with the gluon fusion production cross section at $\sqrt{s} = 7$ TeV $\sigma_{\rm GF}$, $r_{\rm BR}^X \equiv {\rm BR}(\theta_a \to X)/{\rm BR}(h_{\rm SM} \to X)$, $R_X \equiv r_{\rm GF} \times r_{\rm BR}^X$. The branching ratios and 7 TeV LHC production cross section for the SM Higgs are taken from Ref. [36].

$N_{\rm TC}$	$m_{\theta_a} = 449\sqrt{\frac{3}{N_{\rm TC}}}$ [GeV]	$\Gamma_{\rm tot}^{\theta_a}$ [GeV]	${\rm BR}_{gg}$	${\rm BR}_{gZ}$	${\rm BR}_{g\gamma}$	${\rm BR}_{t\bar{t}}$
3	449	23	1.4×10^{-2}	3.1×10^{-5}	1.2×10^{-4}	9.8×10^{-1}
4	389	14	2.5×10^{-2}	5.3×10^{-5}	2.2×10^{-4}	9.7×10^{-1}
	$r_{\rm GF}$	$r_{\rm BR}^{gg}$	$r_{\rm BR}^{t\bar{t}}$	$R_{t\bar{t}}$		
3	51	12	5.1	234		
4	91	20	7.4	625		

$$\begin{aligned}
\Gamma(\theta_a \to gg) &= \frac{5N_{\rm TC}^2 \alpha_s^2 G_F m_{\theta_a}^3}{48\sqrt{2}\pi^3}, \\
\Gamma(\theta_a \to Zg) &= \frac{N_{\rm TC}^2 \alpha_{\rm EM} \alpha_s G_F m_{\theta_a}^3 s^2}{72\sqrt{2}\pi^3 c^2}\left(1 - \frac{m_Z^2}{m_{\theta_a}^2}\right)^3, \\
\Gamma(\theta_a \to \gamma g) &= \frac{N_{\rm TC}^2 \alpha_{\rm EM} \alpha_s G_F m_{\theta_a}^3}{72\sqrt{2}\pi^3}, \\
\Gamma(\theta_a \to q\bar{q}) &= \frac{G_F m_{\theta_a} m_q^2}{\sqrt{2}\pi}\left(1 - \frac{4m_q^2}{m_{\theta_a}^2}\right)^{1/2}.
\end{aligned} \tag{57}$$

The total width and branching ratios at $m_{\theta_a} = 449\ {\rm GeV}\sqrt{3/N_{\rm TC}}$ are shown in Table III for $N_{\rm TC} = 3, 4$. The GF dominates in the θ_a production process at the LHC, yielding the production cross section enhanced by the QCD color factor $(N_c^2 - 1)$ and technifermion loop contributions to be larger than that of the SM Higgs by about a factor of 10^2:

$$\begin{aligned}
\frac{\sigma(gg \to \theta_a)}{\sigma(gg \to h_{\rm SM})} &= (N_c^2 - 1) \times \frac{\Gamma(\theta_a \to gg)}{\Gamma(h_{\rm SM} \to gg)} \\
&\approx 8(N_c^2 - 1)\left(\frac{N_{\rm TC}}{3}\right)^2,
\end{aligned} \tag{58}$$

where $N_c = 3$ and heavy quark mass limit for top and bottom quarks has been taken. The θ_a almost completely decays to $t\bar{t}$ pair with the partial decay rate $\Gamma(\theta_a \to t\bar{t}) \times (\simeq \Gamma_{\theta_a}^{\rm tot})|_{449\ {\rm GeV}} \simeq 23(14)$ GeV for $N_{\rm TC} = 3(4)$, which is comparable to that of the SM Higgs at the same mass. In spite of the large decay rate to $t\bar{t}$, the total width is small enough to treat the θ_a to be a narrow resonance. The θ_a is thus expected to give a large and sharp resonant contribution to the LHC $t\bar{t}$ events.

The θ_a contribution to the $t\bar{t}$ total cross section at $\sqrt{s} = 7$ TeV in the narrow width approximation is estimated at the mass $m_{\theta_a} = 449$ GeV for $N_{\rm TC} = 3$ to be

$$\begin{aligned}
\sigma_{t\bar{t}}^{\theta_a}\Big|_{m_{\theta_a}=449{\rm GeV}} &\approx \sigma_{\rm GF}(pp \to \theta_a) \times {\rm BR}(\theta_a \to t\bar{t})\Big|_{m_{\theta_a}=449{\rm GeV}} \\
&\simeq 60\,{\rm pb},
\end{aligned} \tag{59}$$

which is somewhat too large, yielding 30% of the presently observed cross section $\sigma_{\rm t\bar{t}} \simeq 180$ pb with the accuracy about 13% [38]. The current LHC data on the $t\bar{t}$ cross section thus require the θ_a mass to be below the threshold for the top quark pair, namely, $N_{\rm TC} \geq 6$.

Another interesting discovery channel for the θ_a would be the $\theta_a \to gZ/\gamma$ mode [39]. The cross section may be evaluated by assuming the GF dominance and taking the narrow width approximation:

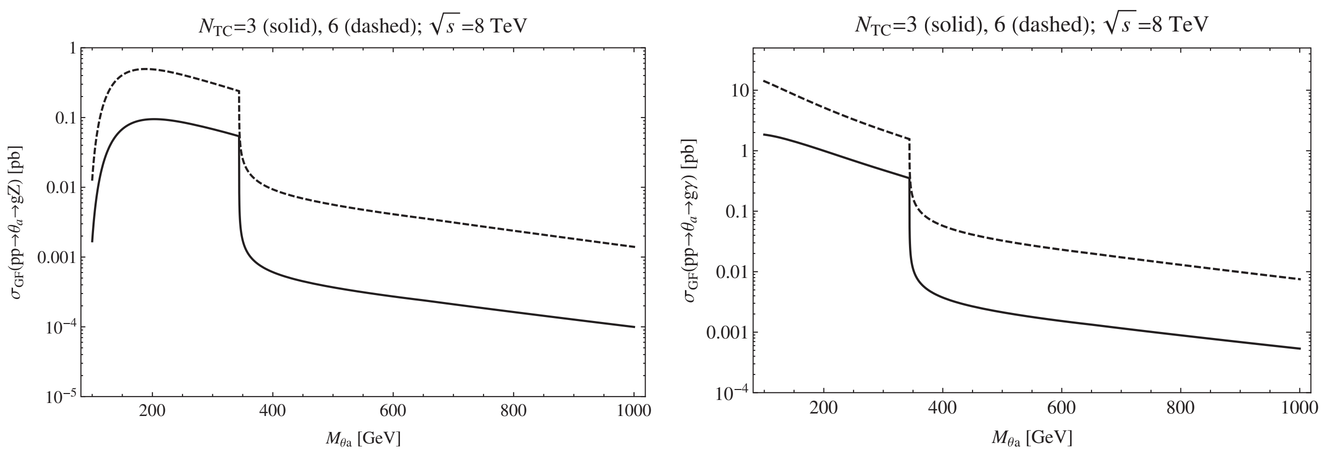

FIG. 5. The predicted θ_a contribution to the LHC cross sections $\sigma(pp \to gZ)$ (left panel) and $\sigma(pp \to g\gamma)$ (right panel) as a function of the θ_a mass for $N_{\rm TC} = 3$ (solid) and 6 (dashed) with $\sqrt{s} = 8$ TeV fixed, in units of pb.

$$\sigma_{\rm GF}(pp\to\theta_a\to gZ/\gamma)$$
$$\approx\sigma_{\rm GF}(pp\to\theta_a)\times{\rm BR}(\theta_a\to gZ/\gamma)$$
$$=\frac{32\pi^2}{s}\int d\eta f_{g/P}(\sqrt{\tau}e^{\eta},m_{\theta_a}^2)f_{g/P}$$
$$\times(\sqrt{\tau}e^{-\eta},m_{\theta_a}^2)\cdot\mathcal{C}_{Z/\gamma}\cdot\frac{\Gamma(\theta_a\to gg){\rm BR}(\theta_a\to gZ/\gamma)}{m_{\theta_a}}, \tag{60}$$

with a pseudorapidity η cut fiducially at $|\eta| = 2.5$ [40] and the parton distribution function $f_{g/P}$ from CTEQ6 [41]. Here $\mathcal{C}_{Z/\gamma}$ denotes the multiplication factor for the initial, resonance, and final states for the partonic cross section, i.e., $\mathcal{C}_{Z/\gamma} = (\frac{1}{8}\cdot\frac{1}{8})_{gg}\times(8)_{\theta_a}\times(\frac{1}{8}\cdot\frac{1}{3}(\frac{1}{2}))_{gZ/\gamma}$. In Fig. 5 the predicted cross section is plotted as a function of the θ_a mass m_{θ_a}. For the reference value $m_{\theta_a} = 449\ {\rm GeV}\sqrt{3/N_{\rm TC}}$ with $N_{\rm TC} = 6$, the expected total number of the $gZ(\gamma)$ events will roughly be a few (ten) thousands for 5 ${\rm fb}^{-1}$ data at $\sqrt{s} = 8$ TeV. The estimate of SM background and significance for the discovery will be pursued in another publication.

IV. SUMMARY

We have explicitly computed the technipion masses in the Farhi-Susskind one-family model taking into account essential features of walking TC. The explicit estimate of the masses was done by using recent results on a nonperturbative analysis based on the ladder Schwinger-Dyson equation employed in a modern version of walking TC.

The charged pion masses were calculated by evaluating one-EW gauge boson exchange diagrams, to show that the collected contributions take the form of integral over the momentum square Q^2 with respect to difference between vector and axial-vector current correlators $\Pi_{V\text{-}A}$, similarly to the computation for charged pion mass in QCD. The EW gauge boson contributions were shown to dramatically cancel each other, so that there are no sizable corrections to the masses, although the $\Pi_{V\text{-}A}$ is quite sensitive to the walking dynamics.

In contrast, sizable corrections were seen in the one-gluon exchange diagram yielding the colored technipion masses. We found that the size of correction is actually enhanced by a large logarithmic factor $\log\Lambda_{\rm TC}/F_\pi$ compared to the naive scale-up version of TC. This is due to the characteristic ultraviolet scaling of $\Pi_{V\text{-}A}$ in the walking TC, which can be seen in the asymptotic form of $\Pi_{V\text{-}A}$ for the ultraviolet region through the slow damping behavior, $\Pi_{V\text{-}A}\sim 1/Q^{4-2\gamma_m}$.

We also evaluated an ETC-induced four-fermion interaction breaking separate chiral symmetry between techniquarks and technileptons, which gives the masses to technipions coupled to the separate chiral currents. The masses were shown to be enhanced due to the chiral condensate enhanced by the large anomalous dimension.

It then turned out that all the technipions are on the order of several hundred GeV (see Table I).

Based on our estimation, we finally discussed the phenomenological implications to the LHC signatures, focusing on neutral isosinglet technipions (P^0 and θ_a), in comparison with the SM Higgs. We found the characteristic LHC signatures can be seen through excessive top quark productions for both two technipions. More on the technipion LHC studies is to be pursued in the future.

ACKNOWLEDGMENTS

This work was supported by the JSPS Grant-in-Aid for Scientific Research Grants No. (S) #22224003, No. (C) #23540300 (K. Y.), and No. #23-01781 (J. J.). J. J. is also supported by the JSPS Postdoctoral Fellowships for Foreign Researchers P11781.

Note added.—After submitting the manuscript, we have found [42] that there exists a massless limit of technidilaton in a holographic model which is a deformation of the model successful for the ordinary QCD with $\gamma_m \simeq 0$ to the walking case with $\gamma_m = 1$. Hence the light technidilaton with 125 GeV is naturally realized so that the technipions are heavier than the technidilaton as described in this paper. Moreover [42], the mass of techni-ρ/a_1 was estimated as $\simeq$ 3.5 GeV (compared with the ladder estimate $\simeq$ 1.5 GeV [43]), which then would not affect our analysis of the technipions in this paper. We also noted that the holographic result is qualitatively different from the ladder one used in this paper in the sense that the former has a massless technidilaton limit, while the latter does not. Nevertheless, the phenomenological output of the holographic model turned out to be similar to the ladder one, and both approaches are consistent with the current LHC data as far as the technidilaton mass is 125 GeV. Hence the numerical estimate in the ladder approximation used in this paper will be roughly the case also in the holographic model.

APPENDIX: TECHNIDILATON ϕ

In this Appendix we shall briefly address the phenomenological contributions to technidilaton signatures coming from the technipion couplings.

From Eq. (1) we read off the technidilaton couplings to the SM particles and technipions. The formulas for decays to the SM particles were previously reported in Refs. [21–23]. While the partial width for two-body decay to technipions is calculated as

$$\Gamma(\phi\to P^AP^B) = \delta^{AB}\frac{M_\phi^3}{32\pi F_\phi^2}\left(1-\frac{4m_{P^A}^2}{M_\phi^2}\right)^{1/2}, \tag{A1}$$

where A, B denote labels of technipions used as in Table I and we have set $\gamma_m \simeq 1$. In deriving Eq. (A1), we added the appropriate technipion mass terms in Eq. (1).

Combining Eq. (A1) with the previously reported ones for the SM particles and using $m_F = 319\ {\rm GeV}\sqrt{\frac{3}{N_{\rm TC}}}$ and

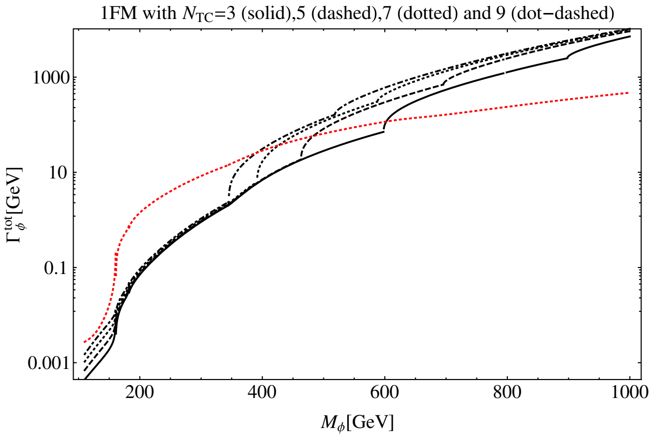

FIG. 6 (color online). The total width of technidilaton as a function of M_ϕ in units of GeV drawn by black solid ($N_{TC} = 3$), dashed ($N_{TC} = 4$), dotted ($N_{TC} = 5$), and dot-dashed ($N_{TC} = 6$) curves, in comparison with that of the SM Higgs (red dotted curve). Use has been made of the reference values of technipion masses listed in Table I for $\Lambda_{TC} = 10^3$ TeV.

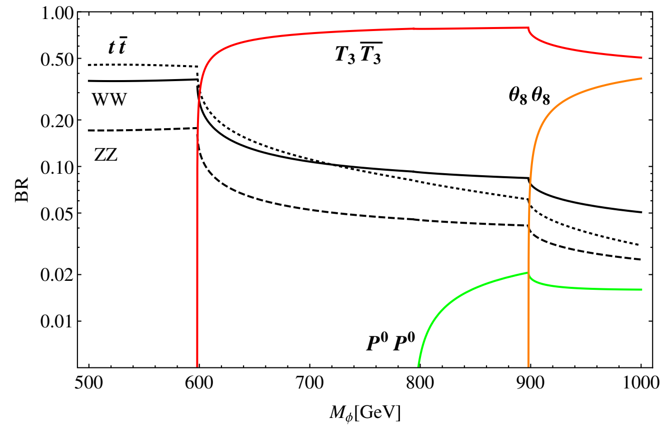

FIG. 7 (color online). The technidilaton branching fraction for the higher mass range $500 \le M_\phi \le 1000$ GeV. The number of TC N_{TC} and Λ_{TC} have been taken to be 3 TeV and 10^3 TeV, respectively. The color-triplet (T_c^i, T_c) and -octet (θ_a^i, θ_a) technipions are collectively expressed as T_3 and θ_8, respectively. The technipion masses are set to the reference values listed in Table I.

$F_\phi = 383\ \text{GeV}(\frac{600\ \text{GeV}}{M_\phi})$ [21–23], in Fig. 6 we plot the total width as a function of M_ϕ with $N_{TC} = 3$ taken, in comparison with the SM Higgs case. The reference values of technipion masses listed in Table I have also been used. Looking at this figure, we see that the total width becomes much larger than that of the SM Higgs at around 500 GeV. This happens because the decay channel for color-triplet technipion pair starts to be kinematically allowed.

The branching fraction in fact becomes dramatically changed above around 500 GeV since a new decay channel to the lightest technipion $T_c \bar{T}_c$ pair (see Table I) starts to open to be dominant. In Fig. 7 we show the branching fraction for mass range $500 \le M_\phi \le 1000$ GeV taking $N_{TC} = 3$ and $\Lambda_{TC} = 10^3$ TeV. For the associated LHC signatures of technidilaton, see Refs. [21–23].

[1] S. Weinberg, Phys. Rev. D **13**, 974 (1976); L. Susskind, Phys. Rev. D **20**, 2619 (1979).
[2] E. Farhi and L. Susskind, Phys. Rep. **74**, 277 (1981).
[3] For other reviews, see, e.g., K. Yamawaki, arXiv:hep-ph/9603293; C. T. Hill and E. H. Simmons, Phys. Rep. **381**, 235 (2003); **390**, 553(E) (2004); F. Sannino, Acta Phys. Pol. B **40**, 3533 (2009).
[4] K. Yamawaki, M. Bando, and K. Matumoto, Phys. Rev. Lett. **56**, 1335 (1986); M. Bando, T. Morozumi, H. So, and K. Yamawaki, Phys. Rev. Lett. **59**, 389 (1987); M. Bando, K. Matumoto, and K. Yamawaki, Phys. Lett. B **178**, 308 (1986).
[5] B. Holdom, Phys. Rev. D **24**, 1441 (1981).
[6] V. A. Miransky, Nuovo Cimento Soc. Ital. Fis. A **90**, 149 (1985).
[7] T. Akiba and T. Yanagida, Phys. Lett. B **169**, 432 (1986); T. W. Appelquist, D. Karabali, and L. C. R. Wijewardhana, Phys. Rev. Lett. **57**, 957 (1986); Work without concept of anomalous dimension was also done earlier based on the pure numerical analysis, see B. Holdom, Phys. Lett. **150B**, 301 (1985).
[8] S. Dimopoulos and L. Susskind, Nucl. Phys. **B155**, 237 (1979).
[9] E. Eichten and K. D. Lane, Phys. Lett. **90B**, 125 (1980).
[10] V. A. Miransky and K. Yamawaki, Phys. Rev. D **55**, 5051 (1997); **56**, 3768(E) (1997).
[11] V. A. Miransky, M. Tanabashi, and K. Yamawaki, Phys. Lett. B **221**, 177 (1989); Mod. Phys. Lett. A **04**, 1043 (1989); Y. Nambu, Enrico Fermi Institute Report No. EFI-89-08, 1989 (unpublished); W. J. Marciano, Phys. Rev. Lett. **62**, 2793 (1989); Phys. Rev. D **41**, 219 (1990); W. A. Bardeen, C. T. Hill, and M. Lindner, Phys. Rev. D **41**, 1647 (1990).
[12] V. A. Miransky and K. Yamawaki, Mod. Phys. Lett. A **04**, 129 (1989).
[13] K. Matumoto, Prog. Theor. Phys. **81**, 277 (1989); T. Appelquist, M. Einhorn, T. Takeuchi, and L. C. R. Wijewardhana, Phys. Lett. B **220**, 223 (1989).
[14] T. Appelquist and G. Triantaphyllou, Phys. Lett. B **278**, 345 (1992); R. Sundrum and S. D. H. Hsu, Nucl. Phys. **B391**, 127 (1993); T. Appelquist and F. Sannino, Phys. Rev. D **59**, 067702 (1999).

[15] M. Harada, M. Kurachi, and K. Yamawaki, Prog. Theor. Phys. **115**, 765 (2006).
[16] M. Kurachi and R. Shrock, Phys. Rev. D **74**, 056003 (2006); M. Kurachi, R. Shrock, and K. Yamawaki, Phys. Rev. D **76**, 036003 (2007).
[17] G. Cacciapaglia, C. Csaki, C. Grojean, and J. Terning, Phys. Rev. D **71**, 035015 (2005); R. Foadi, S. Gopalakrishna, and C. Schmidt, Phys. Lett. B **606**, 157 (2005); R. S. Chivukula, E. H. Simmons, H.-J. He, M. Kurachi, and M. Tanabashi, Phys. Rev. D **72**, 015008 (2005).
[18] W. E. Caswell, Phys. Rev. Lett. **33**, 244 (1974); T. Banks and A. Zaks, Nucl. Phys. **B196**, 189 (1982).
[19] K. D. Lane and M. V. Ramana, Phys. Rev. D **44**, 2678 (1991).
[20] T. Appelquist, J. Terning, and L. C. Wijewardhana, Phys. Rev. Lett. **77**, 1214 (1996); T. Appelquist, A. Ratnaweera, J. Terning, and L. C. Wijewardhana, Phys. Rev. D **58**, 105017 (1998).
[21] S. Matsuzaki and K. Yamawaki, Prog. Theor. Phys. **127**, 209 (2012).
[22] S. Matsuzaki and K. Yamawaki, Phys. Rev. D **85**, 095020 (2012).
[23] S. Matsuzaki and K. Yamawaki, Phys. Rev. D **86**, 035025 (2012).
[24] G. Aad *et al.* (ATLAS Collaboration), Phys. Lett. B **710**, 49 (2012); S. Chatrchyan *et al.* (CMS Collaboration), Phys. Lett. B **710**, 26 (2012).
[25] R. S. Chivukula, P. Ittisamai, E. H. Simmons, and J. Ren, Phys. Rev. D **84**, 115025 (2011).
[26] B. Holdom, Phys. Lett. B **198**, 535 (1987).
[27] M. Hashimoto and K. Yamawaki, Phys. Rev. D **83**, 015008 (2011).
[28] M. E. Peskin, Nucl. Phys. **B175**, 197 (1980).
[29] S. Chadha and M. E. Peskin, Nucl. Phys. **B187**, 541 (1981).
[30] H. Pagels and S. Stokar, Phys. Rev. D **20**, 2947 (1979).
[31] J. Wess and B. Zumino, Phys. Lett. B **37**, 95 (1971); E. Witten, Nucl. Phys. **B223**, 422 (1983).
[32] R. Casalbuoni, S. De Curtis, N. Di Bartolomeo, D. Dominici, F. Feruglio, and R. Gatto, Phys. Lett. B **285**, 103 (1992).
[33] M. Soldate and R. Sundrum, Nucl. Phys. **B340**, 1 (1990); R. S. Chivukula, M. J. Dugan, and M. Golden, Phys. Rev. D **47**, 2930 (1993); M. Harada and K. Yamawaki, Phys. Rep. **381**, 1 (2003).
[34] LEP Higgs Working Group for Higgs Boson Searches, ALEPH Collaboration, DELPHI Collaboration, L3 Collaboration, and OPAL Collaboration, arXiv:hep-ex/0107031; T. Aaltonen *et al.* (CDF Collaboration), Phys. Rev. Lett. **103**, 101803 (2009); V. M. Abazov *et al.* (D0 Collaboration), Phys. Lett. B **682**, 278 (2009); G. Aad *et al.* (ATLAS Collaboration), J. High Energy Phys. 06 (2012) 039; S. Chatrchyan *et al.* (CMS Collaboration), J. High Energy Phys. 07 (2012) 143.
[35] ATLAS Collaboration, Report No. ATLAS-CONF-2011-132, 2011 (unpublished).
[36] S. Dittmaier *et al.* (LHC Higgs Cross Section Working Group Collaboration), arXiv:1101.0593; LHC Higgs Cross Section Working Group *et al.*, arXiv:1201.3084.
[37] CMS Collaboration, Report No. CMS PAS TOP-11-009 (unpublished).
[38] S. Chatrchyan *et al.* (CMS Collaboration), Phys. Rev. D **85**, 112007 (2012); G. Aad *et al.* (ATLAS Collaboration), Phys. Lett. B **717**, 89 (2012).
[39] R. S. Chivukula, R. Rosenfeld, E. H. Simmons, and J. Terning, arXiv:hep-ph/9503202.
[40] G. Aad *et al.* (ATLAS Collaboration), arXiv:0901.0512.
[41] J. Pumplin, D. R. Stump, J. Huston, H. L. Lai, P. M. Nadolsky, and W. K. Tung, J. High Energy Phys. 07 (2002) 012.
[42] S. Matsuzaki and K. Yamawaki, Phys. Rev. D **86**, 115004 (2012).
[43] K. Yamawaki, Prog. Theor. Phys. Suppl. **197**, 76 (2012).